Synthesis and Chemistry of a Bridging Vinylidenedicobalt Complex. Evidence for a Nonchain Radical Mechanism in Its Reaction with Metal Hydrides To Give Heteronuclear Clusters

Eric N. Jacobsen and Robert G. Bergman*

Contribution from the Department of Chemistry, University of California, Berkeley, California 94720. *Received July 30, 1984*

Abstract: Reaction of the radical anion species $[CpCo(CO)]_2Na$ with 1,1-dibromoethylene yields the dicobalt bridging vinylidene complex $(\mu\text{-}CCH_2)(CpCoCO)_2$ (**1**), the structure of which was determined crystallographically. Protonation of **1** occurs readily with $HBF_4\cdot OEt_2$, giving the bridging ethylidyne salt $[(\mu\text{-}CCH_3)(CpCoCO)_2]^+BF_4^-$ (**2**). Compound **2** is unstable in solution, decomposing at room temperature to the trinuclear ethylidyne cluster $[(\mu_3\text{-}CCH_3)(Cp_2Co_3(CO)_2)]^+BF_4^-$ (**3**). Reduction of **2** with $NaBH_4$ in THF gives ethylidene complex $(\mu\text{-}CHCH_3)(CpCoCO)_2$ (**4**), which may also be obtained directly from **1** by reaction with H_2 at 60 °C. Compound **1** reacts cleanly with $CpMo(CO)_2(L)H$ (L = CO, PMe_3, PPh_3) in dilute benzene solutions to give heteronuclear cluster $(\mu^3\text{-}CCH_3)(\mu_2\text{-}CO)(CpCo)_2[CpMo(CO)_2]$ (**5**). Similarly, the manganese-containing cluster $(\mu_3\text{-}CCH_3)(CpCo)_2(\mu_2\text{-}CO)_2[Mn(CO)_3]$ (**6**) is formed upon slow addition of a solution of $HMn(CO)_5$ to a dilute solution of **1** at 60 °C. The crystal structures of both **5** and **6** were determined. Kinetics performed on the reactions of **1** with $CpMo(CO)_3X$ (X = H, D) show that the reaction is first order in each reagent and second order overall. The observation of a primary inverse isotope effect k_H/k_D of at least 0.70 suggests a nonchain radical mechanism is operative, involving initial H (D) atom transfer from the molybdenum reagent to **1**. Further evidence for this, as well as for the existence of the resulting radical pair in a solvent cage, is provided by trapping experiments and by a study of the effect of solvent viscosity. Evidence against alternate mechanisms, such as ones involving proton transfer or initial ligand dissociation, is also given.

Although a large number of heteronuclear transition-metal cluster complexes are known, it is presently difficult to design rational syntheses of such materials. Classical "cluster expansion reactions" have relied on mixing together mono- or polynuclear complexes and subjecting them to pyrolysis.[1] However, mechanistic understanding of such reactions is nearly nonexistent, and their predictability is very low. Recently, more rational methods have been devised; these include replacement of one metal fragment by another in preformed clusters[1,2] and displacement (or "redox") reactions involving interactions of nucleophilic metal complexes with electrophilic or coordinatively unsaturated ones.[1] These are somewhat more predictable, but mechanistic understanding of such processes is still very limited.

One of the most potentially general and chemically interesting approaches to building up heteronuclear clusters involves the addition of one metal species to another one which contains a reactive organic or metal–organic function. Stone's group has used this idea in a particularly powerful way in the addition of coordinatively unsaturated metal complexes to metal alkylidene and alkylidyne groups;[3] similar reactions involving alkynylmetal and alkenylmetal substrates have been reported.[4]

Another potentially powerful member of the class of cluster expansion reactions based on the reactivity of metal–organic functional groups involves the addition of an M—X single bond across an unsaturated organic group bound to a smaller cluster; e.g., $M_nA{=}B + M_m{-}H \rightarrow (M_n)(M'_m)A{-}BH$. An example of this type of reaction is the addition of a metal hydride to a dinuclear vinylidene ($M_2C{=}CH_2$) complex,[5] producing a trinuclear alkylidyne cluster product. We are aware of only one example of such a process, which has been used to carry out a heteronuclear cluster expansion reaction leading to a trinuclear Mn–Fe–Fe derivative.[6] In seeking further examples, we recently extended our method for the preparation of dinuclear cobalt complexes[7] to the synthesis of vinylidene species. We found that certain metal hydrides do add across the vinylidene double bond, leading to new heteronuclear clusters, and our preliminary results on this reaction were recently published.[8] The cleanliness of this reaction, and the paucity of information currently available on the mechanisms of any type of cluster expansion, encouraged us to examine it in depth. In this paper we report the full details of the preparative and structural work and the results of a kinetics and mechanism study which strongly implicates radical intermediates in the process.

(1) For a review, see: Gladfelter, W. L.; Geoffroy, G. L. *Adv. Organomet. Chem.* **1980**, *18*, 207.

(2) For some examples, see: (a) Beurich, H.; Vahrenkamp, H. *Chem. Ber.* **1982**, *115*, 2385. (b) Beurich, H.; Blumhofer, R.; Vahrenkamp, H. *Chem. Ber.* **1982** *115*, 2409. (c) Jaouen, G.; Marinetti, A.; Mentzen, B.; Mutin, R.; Saillard, J. Y.; Sayer, B. G.; McGlinchey, M. J. *Organometallics* **1982**, *1*, 753. (d) Mlekuz, M.; Bougeard, P.; McGlinchey, M. J.; Jaouen, G. *J. Organomet. Chem.* **1983**, *253*, 117.

(3) (a) Ashworth, T. V.; Howard, J. A. K.; Laguna, M.; Stone, F. G. A. *J. Chem. Soc., Dalton Trans.* **1980**, 1593. (b) Berry, M.; Howard, J. A. K.; Stone, F. G. A. *Ibid.* **1980**, 1601. (c) Howard, J. A. K.; Mead, K. A.; Moss, J. R.; Navarro, R.; Stone, F. G. A.; Woodward, P. *Ibid.* **1981**, 743. (d) Chetcuti, M. J.; Chetcuti, P. A. M.; Jeffery, J. C.; Mills, R. M.; Mitrprachachon, P.; Pickering, S. J.; Stone, F. G. A.; Woodward, P. *Ibid.* **1982**, 699. (e) Chetcuti, M. J.; Howard, J. A. K.; Mills, R. M.; Stone, F. G. A.; Woodward, P. *Ibid.* **1980**, 1593. (f) Green, M.; Jeffery, J. C.; Porter, S. J.; Razay, H.; Stone, F. G. A. *Ibid.* **1982**, 2475. (g) Busetto, L.; Jeffery, J. C.; Mills, R. M.; Stone, F. G. A.; Went, M. J.; Woodward, P. *Ibid.* **1983**, 101.

(4) See, for example: (a) Ros, J.; Mathieu, R. *Organometallics* **1982**, *2*, 771. (b) Ustynyuk, N. A.; Vinogradova, V. N.; Korneva, V. N.; Slovokhotov, Yu. L.; Struchkov, Yu. T. *Koord. Khim.* **1983**, *9*, 631.

(5) Dinuclear vinylidene complexes have been reported for the following metals. (a) Mn: Folting, K.; Huffman, J. C.; Lewis, L. N.; Caulton, K. G. *Inorg. Chem.* **1979**, *18*, 3483. (b) Fe: Kao, S. C.; Lu, P. P. Y.; Pettit, R. *Organometallics* **1982**, *1*, 911. Dawkins, G. M.; Green, M.; Jeffery, J. C.; Sambale, C.; Stone, F. G. A. *J. Chem. Soc., Dalton Trans.* **1983**, 499. (c) Ru: Colborn, R. E.; davies, D. L.; Dyke, A. F.; Endesfelder, A.; Knox, S. A. R.; Orpen, A. G.; Ploas, D. *Ibid.* **1983**, 2661. (d) Rh: AlObaidi, Y. N.; Green, M.; White, N. D.; Taylor, G. E. *Ibid.* **1982**, 319. (e) FeMn: Kolobova, N. E.; Ivanov, L. L.; Zhivanko, O. S.; Aleksandrov, G. G.; Struchkov, Yu. T. *J. Organomet. Chem.* **1982**, *288*, 265. (f) Pt: Afzal, D.; Lenhard, P. G.; Lukehart, C. M. *J. Am. Chem. Soc.* **1984**, *106*, 3050. (g) Mono- and dihalo-substituted (μ-butenolido)(μ-vinylidene)hexacarbonyl dicobalt complexes have been reported: Hovarth, I. T.; Palyi, G.; Marko, L.; Andreetti, G. D. *Inorg. Chem.* **1983**, *22*, 1049. For a recent review on vinylidene and propadienylidene complexes, see: (h) Bruce, M. I.; Swincer, A. G. *Adv. Organomet. Chem.* **1983**, *22*, 59.

(6) Brun, P.; Dawkins, G. M.; Green, M.; Mills, R. M.; Salaun, J.-Y.; Stone, F. G. A.; Woodward, P. *J. Chem. Soc., Dalton Trans.* **1983**, 2661.

(7) (a) Schore, N. E.; Ilenda, C. S.; Bergman, R. G. *J. Am. Chem. Soc.* **1976**, *98*, 7436. (b) White, M. A.; Bergman, R. G. *J. Chem. Soc., Chem. Commun.* **1979**, 1056. (c) Bergman, R. G. *Acc. Chem. Res.* **1980**, *13*, 113. (d) Theopold, K. H.; Bergman, R. G. *Organometallics* **1982**, *1*, 1571. (e) Theopold, K. H.; Bergman, R. G. *J. Am. Chem. Soc.* **1983**, *105*, 464. (f) Schore, N. E.; Ilenda, C. S.; White, M. A.; Bryndza, H. E.; Matturro, M. G.; Bergman, R. G. *Ibid.* **1984**, *106*, 7451.

(8) Jacobsen, E. N.; Bergman, R. G. *Organometallics* **1984**, *3*, 329.

0002-7863/85/1507-2023$01.50/0

Scheme I

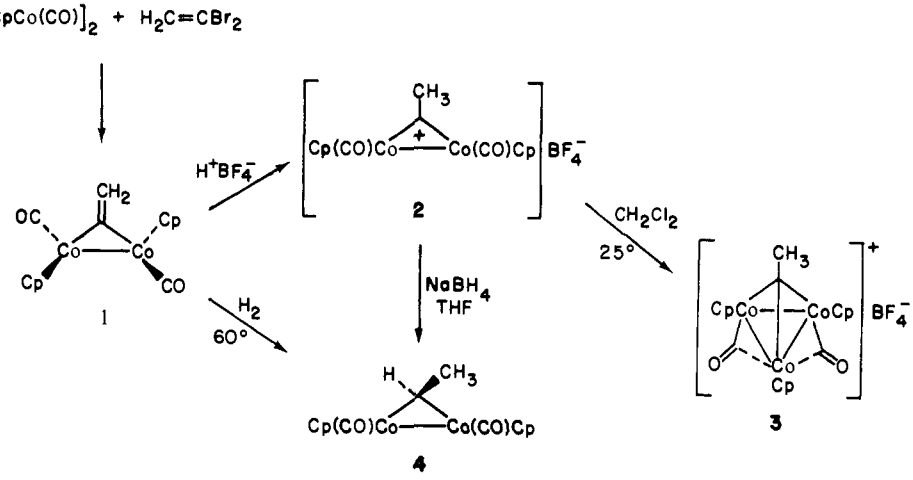

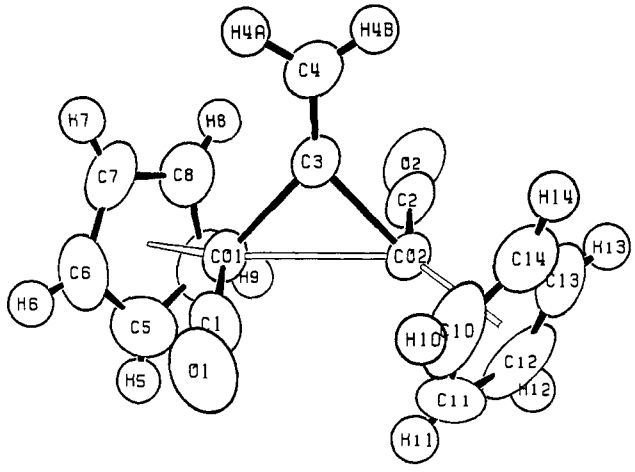

Figure 1. ORTEP drawing of one molecule of **1**, showing the atomic labeling scheme. Thermal ellipsoids are scaled to represent the 50% probability surface.

Synthesis and Reactions of Dinuclear Vinylidene Complex 1

Preparation and Structure of 1. As we have previously reported, the dinuclear radical anion $Na[CpCo(CO)]_2$ reacts with a variety of 1,*n*-dihalides to afford $[CpCo(CO)]_2$ and dicobaltacycles of different ring sizes.[7d,e] In all the reported cases, however, the dihalides have been sp^3 hybridized at the halogen-substituted carbon(s). We have now found that the same type of reaction also occurs at the vinyl disubstituted carbon of the oxygen-sensitive alkene 1,1-dibromoethylene[9] to give the title bridging vinylidene complex **1** (Scheme I). Purification by air-free chromatography followed by recrystallization from hexane gave large dark crystals of a material with spectroscopic and analytical properties consistent with **1**. Complex **1** was isolated in 24% yield based on $Na[CpCo(CO)]_2$, or 48% of the theoretical yield, since 1 equiv of the neutral dimer $[CpCo(CO)]_2$ is produced in the reaction. The structure of the vinylidene complex was confirmed by an X-ray diffraction study, as reported in the preliminary communication;[8] an ORTEP of the molecule is illustrated in Figure 1. The molecule is virtually identical with the analogous bridging methylene complex in its geometry about the cobalt centers, with the Cp's in a trans disposition and the CO's terminal and nearly perpendicular to the Co–Co bond. Similar to other known compounds of this type, the geometry at the vinylidene double bond is close to planar (3° twist angle) and the C–C bond is rather short.

Protonation of 1 by HBF_4. Earlier studies on dinuclear complexes related to vinylidene **1** have demonstrated that interaction with the metal centers can help stabilize a charge on a bridging carbon atom.[5,10] Consistent with this pattern, **1** reacts cleanly with HBF_4 in ether solution to give the bridging ethylidyne dicobalt complex **2** in nearly quantitative yield (Scheme I). In this reaction, **2** precipitates out of solution as an analytically pure powder within seconds after addition of HBF_4 to **1**. Cationic ethylidyne complex **2** is quite stable under nitrogen in the solid state, but attempts to dissolve it in common polar solvents such as acetonitrile, acetone, dimethyl sulfoxide, or water all resulted in rapid decomposition. In methylene chloride, solutions of **2** are stable at −78 °C for several hours and at room temperature for a few minutes.

Ethylidyne complex **2** was characterized by elemental analysis and FAB mass spectrometry, as well as by ^1H NMR and solution IR. The IR spectrum shows two high-frequency absorbances (2060, 2033 cm^{-1}) and one low one (1884, br), indicating that isomers containing both terminal and bridging carbonyls are probably present in solution.

Decomposition of **2** in methylene chloride at room temperature is quite clean, affording the trinuclear cluster **3** within an hour. Cluster **3** was isolated in 82% yield based on cobalt; evidence for this structure was drawn from its analytical and spectral properties, most notably by the close similarity of its IR spectrum to those of $(\mu_3\text{-CH})[Cp_3M_3(CO)_2]^+BF_4^-$ (M = Co, Rh), both of which have been characterized crystallographically.[11] The CO absorbances for all three compounds are at noticeably high frequency (1910, 1870 cm^{-1} for **3**), reflecting both the cationic charge on the cluster and the semibridging nature of the ligands. Decomposition of **2** in the polar donor solvents mentioned above also yields **3**, although much less cleanly.

A suspension of ethylidyne **2** in THF reacts rapidly with $NaBH_4$ to give the bridging ethylidene complex **4** in 34% yield. The conversion of **1** to **4** can also be accomplished directly by reaction of **1** with H_2 at 60 °C (43% yield). This is the first reported case of hydrogenation of a μ-vinylidene double bond, and it offers an interesting indication of how the reactivity of the organic π-system is enhanced due to interaction with the metals. Compound **4** is unstable to the reaction conditions under which it is formed, reacting further with H_2 to give ethane, ethylene, and the usual cobalt containing side products ($CpCo(CO)_2$ and clusters).

Cluster-Forming Reactions. When a dilute solution (2.5×10^{-3} M) of **1** and $CpMo(CO)_3H$ was heated in benzene to 60 °C, a color change from deep red to green was observed concurrent with disappearance of starting material. The product, obtained after chromatography on silica followed by recrystallization from benzene/hexane, had spectral and analytical properties consistent with the heteronuclear Co_2/Mo structure **5** (Scheme II). Crystals

(9) Verhulst, J.; van Hemelrijck, F.; Jungers, J. C. *Natuurwet. Tijdschr. (Chent)* **1943**, *25*, 203.

(10) Lewis, L. N.; Huffman, J. C.; Caulton, K. G. *J. Am. Chem. Soc.* **1980**, *102*, 403.

(11) Rh: Herrmann, W. A.; Plank, J.; Riedel, D.; Ziegler, M. L.; Weidenhammer, K.; Guggolz, E.; Balbach, B. *J. Am. Chem. Soc.* **1981**, *103*, 63. Co: Larson, C. E.; Jacobsen, E. N.; Bergman, R. G., unpublished results. The infrared carbonyl frequencies for this cluster in CH_3CN solution are 1912 and 1863 cm^{-1}.

Table I. Crystal and Data Collection Parameters

	1	5	6
	Crystal Parameters at 25 °C		
a, Å	8.2535 (6)	8.3550 (9)	8.6801 (13)
b, Å	9.0316 (8)	8.3561 (9)	13.5654 (13)
c, Å	9.1980 (11)	25.4542 (23)	15.0336 (16)
α, deg	74.427 (8)		84.327 (8)
β, deg	76.745 (8)	91.825 (8)	89.258 (10)
γ, deg	84.514 (7)		77.794 (10)
v, Å^3	642.4 (1)	1776.2 (6)	1721.6 (5)
space group	$P\bar{1}$	$P2_1/c$	$P\bar{1}$
MW, amu	330.12	520.17	470.09
Z	2	4	4
d(calcd), g cm^{-3}	1.71	1.945	1.81
μ(calcd), cm^{-1}	25.67	25.40	26.2
size, mm	0.26 × 0.30 × 0.33	0.12 × 0.22 × 0.43	0.18 × 0.20 × 0.25
	Data Measurement Parameters		
diffractometer	Enraf-Nonius CAD-4		
radiation	Mo K$\bar{\alpha}$ (λ = 0.71073 Å)		
monochromator	highly oriented graphite (2θ m = 12.2°) perpendicular mode, assumed 50% perfect		
detector	crystal scintillation counter, with PHA		
aperture crystal dist, mn	173		
vertical aperture, mm	3.0		
horizontal aperture, mm	2 + 1 tan (θ) (variable)		
reflctns measd	$+h \pm k \pm l$	$+h +k \pm l$	$+h \pm k \pm l$
2θ range, deg	3-55	3-45	3-45
scan type	θ-2θ		
scan speed (θ), deg/min	0.60-6.7		
scan width ($\Delta\theta$)	0.5 + 0.347 tan (θ)		
bkgd	measured over an additional 0.25 ($\Delta\theta$) added to each end of the scan		
reflctns collected	3142	2671	
unique reflctns	2936	2302	4503
std reflctns	(600), (060), (006)	508, 4 11 2, 257	(456), (1 1 10), (452)
orientation	3 reflctns checked after every 250 measurements		

Scheme II

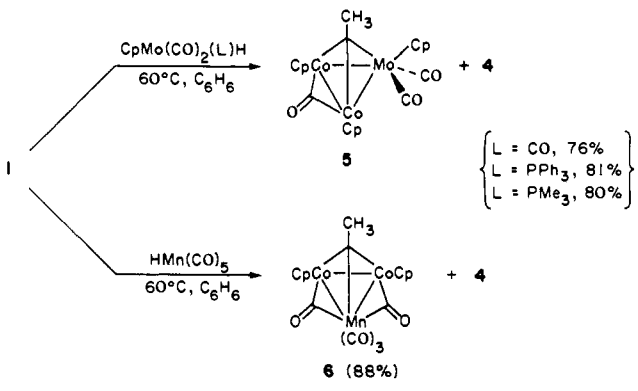

of **5** were isolated in 76% yield under these conditions. Reaction of **1** with the phosphine-substituted derivatives $CpMo(CO)_2(L)H$ (L = PMe_3 or PPh_3) under the dilute conditions described above also afforded cluster **5** in high yield. When any of these reactions was run at higher concentration, the yield of **5** was reduced and hydrogenated dinuclear ethylidene complex **4** was observed as a side product.

Similarly, when **1** and $HMn(CO)_5$ were dissolved in benzene in a 1:1 ratio and heated to 60 °C, the major product was ethylidene **4**, although a small amount of heteronuclear Co_2/Mn cluster **6** was also formed (Scheme II). The yield of **6** was greatly increased by carrying out the reaction using very low concentrations of $HMn(CO)_5$. The most effective method found was to add a solution of $HMn(CO)_5$ to a dilute solution of **1** at 60 °C over several hours by syringe pump. In this manner, after workup similar to the one used for **5**, crystals of **6** were obtained in 88% yield. A detailed discussion on the effect of dilution on these reactions will follow (see Mechanistic Studies section).

Compounds **5** and **6** were both fully characterized by spectroscopic and analytical methods. ^{13}C NMR spectra of both **5** and **6** each show only a single CO resonance, suggesting that in solution both molecules undergo some fluxional process whereby the carbonyl ligands in each become equivalent.[12] This type of fluxionality is well precedented in trinuclear systems.[3d-g] Further evidence that this is the case for **5** and **6** is given by the significant differences between the IR spectra of solutions of the compounds and spectra of solid samples (taken as KBr pellets or Nujol mulls; see Experimental Section).

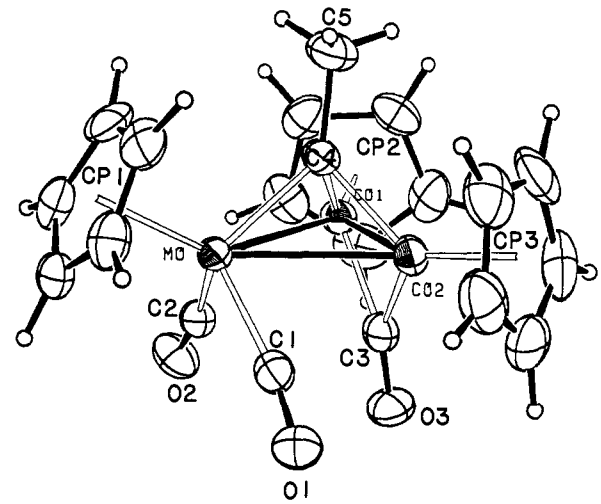

Figure 2. ORTEP drawing of one molecule of **5**.

X-ray Structure Determination of 5 and 6. In order to unambiguously ascertain the positions of the carbonyl ligands in the solid state and, more generally, to gain detailed structural information on these interesting comounds, the structures of both clusters were determined crystallographically. ORTEP diagrams of each molecule are shown in Figures 2 and 3, and selected bond

(12) As suggested by a referee, there exists the possibility that the μ-CO in **5** is broadened and not seen in the ^{13}C NMR spectrum.

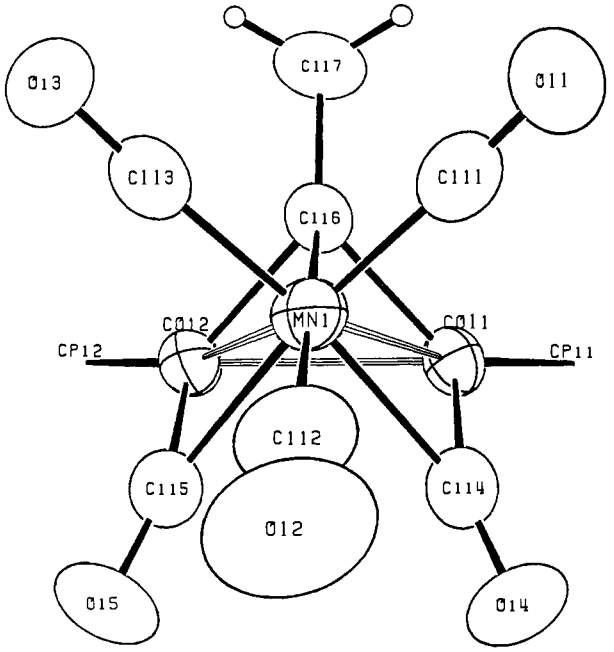

Figure 3. ORTEP drawing of one of the two different molecules of 6. (The other molecule is virtually identical with respect to bond distances and angles.) Cyclopentadienyl rings have been omitted for clarity.

Table II. Selected Distances (Å) and Angles (deg) for Compound **1**

distances			angles			
atom 1	atom 2	distance	atom 1	atom 2	atom 3	angle
CO1	CO2	2.500 (1)	CO2	CO1	C1	90.88 (5)
			CO2	CO1	C3	48.37 (4)
CO1	C1	1.726 (2)	C1	CO1	C3	92.89 (6)
CO1	C3	1.886 (1)	CO1	CO2	C2	90.4 (5)
CO1	CP1	1.716	CO1	CO2	C3	48.50 (4)
			C2	CO2	C3	90.43 (6)
CO2	C2	1.722 (1)	CO1	C3	CO2	83.13 (5)
CO2	C3	1.882 (1)	CO1	C3	C4	137.84 (11)
CO2	CP2	1.724	CO2	C3	C4	138.98 (11)
C3	C4	1.312 (2)	C3	C4	H4A	121.9 (10)
C4	H4A	1.03 (2)	C3	C4	H4B	121.9 (11)
C4	H4B	0.95 (2)	H4A	C4	H4B	115.9 (15)

distances and angles are given in Tables III and IV. Compound **5** crystallizes in the space group $P2_1/c$ with cell dimensions shown in Table I. A carbonyl ligand bridges the two cobalt atoms, with the Mo atom carrying two terminal carbonyls. All three carbonyl ligands lie on the same side of the Co–Co–Mo plane, away from the bridging ethylidyne ligand and the cyclopentadienyl rings. Compound **6** crystallizes in the space group $P\bar{1}$ with cell dimensions given in Table I. Carbonyl ligands in **6** bridge the Co–Mn bonds, with three terminal carbonyls remaining on the Mn atom. This disposition of the ligands results in an octahedral geometry about the Mn, if the metal–metal bonds are ignored.

Attempts to broaden the scope of this reaction using other metal hydride reagents met with little success. Reaction of **1** with $CpCr(CO)_3H$ occurs instantly at room temperature, affording mostly **4**. No Cr–Cr-containing clusters were detected. Conversely, $CpW(CO)_3H$ does not react appreciably with **1**, and prolonged heating of the mixture results only in decomposition of the starting materials.

Mechanism of the Cluster-Forming Reaction

Reactions of **1** with metal hydrides are apparently very sensitive to both the reaction conditions and to the strength of the metal–hydride bond. This led us to examine the reaction of **1** with $CpMo(CO)_3H$ more closely, with the intention of gaining some insight into the mechanism of cluster formation.

Kinetics, Isotope Effect, and Isotope Exchange Studies. Indication of a Radical Mechanism. The kinetics of the reaction were conveniently measured by UV–vis spectroscopy. Spectra taken over time of solutions of **1** with greater than 5-fold excess of $CpMo(CO)_3H$ (pseudo-first-order conditions) at 60 °C gave good isosbestic points at $\lambda = 428$ and 488 nm. In each of five runs with varying concentrations of $CpMo(CO)_3H$, a plot of $\ln I_t - I_\infty$ vs. t gave very good straight lines. The results are shown in Figure 4, in which the apparent pseudo-first-order rate constants for the disappearance of **1** are plotted as a function of $CpMo(CO)_3H$ concentration. A straight line is obtained which passes through the origin, indicating that the reaction is first order in both **1** and $CpMo(CO)_3H$ and second order overall. The second-order rate

Table III. Selected Distances (Å) and Angles (deg) for Complex **5**

distances			angles			
atom 1	atom 2	distance	atom 1	atom 2	atom 3	angle
MO	CO1	2.729 (1)	CO1	MO	CO2	51.76 (1)
MO	CO2	2.726 (1)	CO1	MO	C2	63.78 (6)
CO1	CO2	2.381 (1)	CO2	MO	C1	63.70 (6)
			CP1[a]	MO	CO1	141.73
C4	MO	2.032 (2)	CP1	MO	C4	113.61
C4	CO1	1.893 (2)	C1	MO	C2	91.87 (8)
C4	CO2	1.898 (2)	C1	MO	C4	107.16 (8)
C4	C5	1.507 (3)	C2	MO	C4	107.05 (8)
MO	C1	1.974 (2)	MO	CO1	CO2	64.05 (1)
MO	C2	1.984 (3)	CP2	CO1	C4	131.45
CO1	C3	1.882 (2)	MO	CO2	CO1	64.20 (1)
CO2	C3	1.880 (2)	CP3	CO2	C4	132.06
C1	O1	1.155 (3)				
C2	O2	1.145 (3)	MO	C1	O1	170.08 (18)
C3	O3	1.177 (2)	MO	C2	O2	169.77 (19)
			CO1	C3	O3	140.59 (19)
MO	CP1[a]	2.019	CO2	C3	O3	140.62 (18)
CO1	CP2[a]	1.717	CO1	C3	CO2	78.50 (9)
CO2	CP3[a]	1.715				
			MO	C4	CO1	88.05 (8)
			MO	C4	CO2	87.77 (8)
			CO1	C4	CO2	77.82 (8)
			MO	C4	C5	133.22 (15)
			CO1	C4	C5	126.81 (6)
			CO2	C4	C5	125.68 (16)

[a] Geometric centroids of the cyclopentadiene rings.

Table IV. Selected Distances (Å) and Angles (deg) for One of the Two Complete Molecules of **6**[a]

distances			angles			
atom 1	atom 2	distance	atom 1	atom 2	atom 3	angle
MN1	CO11	2.499 (1)	CO11	MN1	C114	45.92 (7)
MN1	CO12	2.515 (1)	CO11	MN1	C116	48.23 (8)
CO11	CO12	2.490 (1)	CO12	MN1	C115	45.62 (8)
			CO12	MN1	C116	48.14 (8)
MN1	C111	1.813 (3)				
MN1	C112	1.826 (3)	C111	MN1	C112	93.61 (15)
MN1	C113	1.805 (3)	C111	MN1	C113	90.85 (13)
MN1	C114	2.106 (3)	C111	MN1	C114	96.77 (11)
MN1	C115	2.126 (3)	C111	MN1	C115	172.24 (12)
CO11	C114	1.832 (3)	C111	MN1	C116	90.02 (12)
CO12	C115	1.834 (3)	C112	MN1	C113	94.79 (14)
			C112	MN1	C114	83.27 (12)
MN1	C116	1.922 (3)	C112	MN1	C115	82.46 (14)
CO11	C116	1.881 (3)	C112	MN1	C116	175.70 (13)
CO12	C116	1.889 (2)	C113	MN1	C114	172.23 (11)
C117	C116	1.508 (4)	C113	MN1	C115	96.13 (12)
			C113	MN1	C116	87.46 (12)
CO11	CP11	1.720 (1)	C114	MN1	C115	76.18 (10)
CO12	CP12	1.724 (1)	C114	MN1	C116	94.02 (11)
			C115	MN1	C116	93.66 (11)
C111	O11	1.142 (3)				
C112	O12	1.142 (4)	CO12	CO11	C116	48.79 (8)
C113	O13	1.144 (3)	CO11	CO12	C116	48.54 (8)
C114	O14	1.165 (3)				
C115	O15	1.159 (3)	MN1	C114	CO11	78.43 (11)
			MN1	C115	CO12	78.46 (11)
			MN1	C116	C117	133.10 (20)
			CO11	C116	C117	129.03 (20)
			CO12	C116	C117	129.12 (20)

[a] The data for the other molecule are very similar. They are included in the supplementary material.

Scheme III

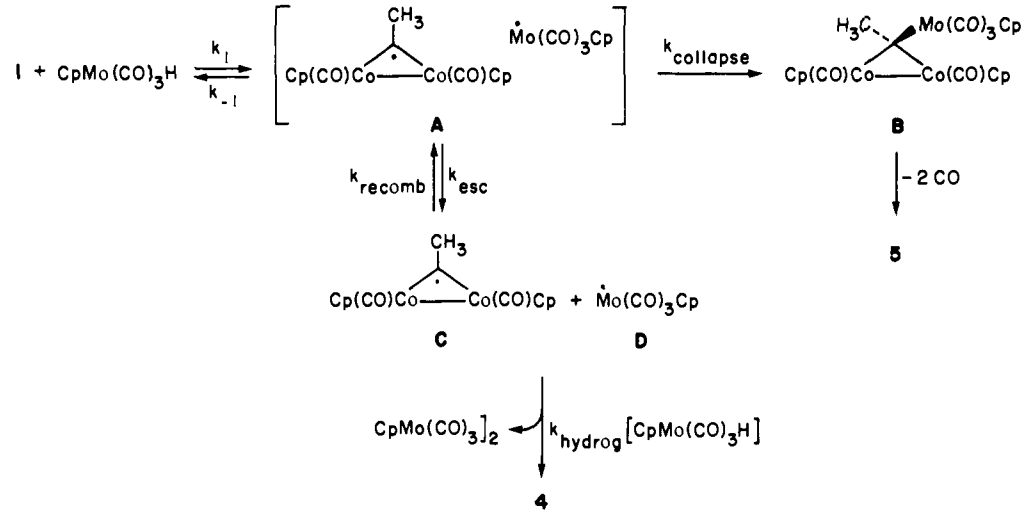

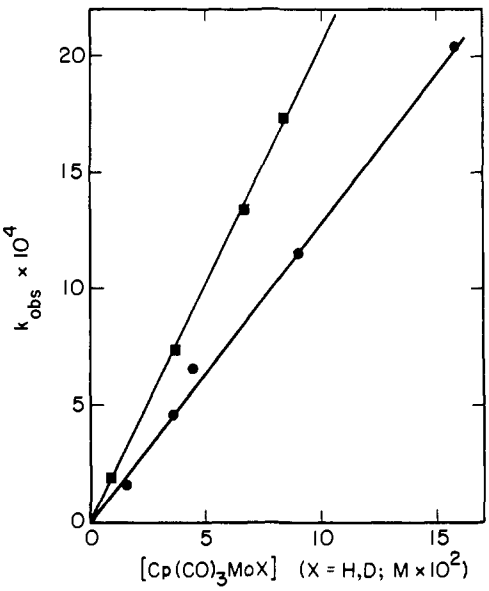

Figure 4. k_{obsd} vs. concentration plot, for the reaction of **1** with $CpMo(CO)_3X$ (X = H, D) at 60 °C, (●) X = H, (■) X = D.

constant k_H is 1.30×10^{-2} M^{-1} s^{-1}.

Kinetics of the reaction of **1** with $CpMo(CO)_3D$ were measured in a similar manner, and the data are also plotted in Figure 4. The second-order rate constant k_D for this reaction is 2.06×10^{-2} M^{-1} s^{-1}, so there is a significant *inverse* isotope effect in the reaction of **1** with $CpMo(CO)_3X$ (X = H, D) of $k_H/k_D = 0.63$. This result is reminiscent of that obtained in the reactions of $HMn(CO)_5$ and $CpMo(CO)_3H$ with α-methylstyrene[13] and is general for reactions in which the first step involves cleavage of a weak bond to H (or D)[14] and formation of a stronger bond to the same H(D). A mechanism for the formation of **5** which involves such a process is outlined in Scheme III. The first step involves hydrogen atom transfer from $CpMo(CO)_3H$ to **1**, whereby a Mo–H bond is broken and a C–H bond is formed giving the radical pair A. Collapse of the radical pair gives intermediate B, which then can lose two CO ligands to form cluster **5**. The inverse isotopic effect in such a mechanism arises from the fact that the new (higher frequency) C–H bond in A is stronger than the initial (lower frequency) Mo–H bond. Thus the preequilibrium ratio [A]/[**1**][$CpMo(CO)_3X$] is greater for X = D than for X = H. The higher relative concentration of the reactive intermediate results in a faster rate of reaction.

Scheme IV

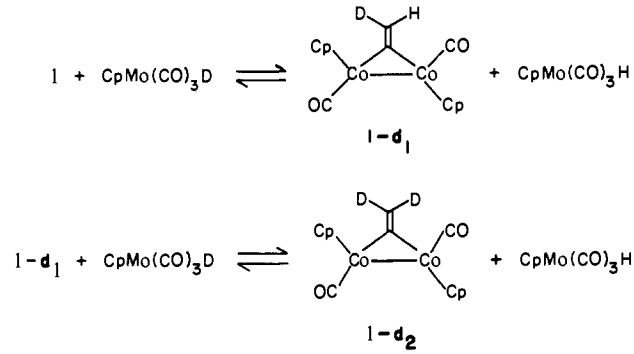

If the nonchain radical mechanism in Scheme III is indeed operative, then the first step must be rapidly reversible in order to see an equilibrium effect; the rate-determining transition state of the reaction is reached *after* the formation of radical pair A. This is in fact the case, since in the reaction of **1** with excess $CpMo(CO)_3D$, ^1H NMR spectra taken at early reaction times show formation of $CpMo(CO)_3H$ and **1**-d_2 (Scheme IV) at least 100 times faster than cluster formation. This exchange is fast even at −40 °C (toluene-d_8), and attempts to obtain exact rate data by NMR were not successful. Nonetheless, it is clear that the necessary equilibration does in fact occur.

As a result of this rapid equilibration, the interpretation of our kinetic isotope effect study on the reaction of **1** with $CpMo(CO)_3H$ and $CpMo(CO)_3D$ must be modified partially. Each rate measurement was carried out by using a large excess of molybdenum hydride or deuteride, in order to maintain pseudo-first-order conditions. Thus, in the experiments using $CpMo(CO)_3D$, the hydrogens on the terminal vinylidene carbon must have been essentially completely exchanged for deuterium almost immediately (certainly before a significant amount of conversion to product has occurred); because of the excess molybdenum deuteride present, the metal must still have contained largely deuterium as well. Thus the rate study provides a combined primary (due to metal–H (D) cleavage) and secondary (due to changes in the vibration frequencies of the two H's (D's) attached to the vinylidene carbon) isotope effect, rather than simply the primary effect discussed earlier. Fortunately, Pryor and his co-workers have measured secondary isotope effects for reactions of this type, in which an organic radical adds to an sp^2 carbon of an alkene, converting it to the sp^3 carbon of a new radical.[15] These secondary

(13) Sweany, R. L.; Halpern, J. *J. Am. Chem. Soc.* **1977**, *99*, 8335. Sweany, R. L.; Butler, S. C.; Halpern, J. *J. Organomet. Chem.* **1981**, *213*, 487. Sweany, R. L.; Comberrel, D. S.; Dombourian, M. F.; Peters, N. A. *J. Organomet. Chem.* **1981**, *216*, 57.

(14) Bell, R. P. *Chem. Soc. Rev.* **1974**, *3*, 513.

(15) Henderson, R. W.; Pryor, W. A. *Int. J. Chem. Kinet.* **1972**, *4*, 325. For a review of secondary isotope effects, see: Halevi, E. A. *Prog. Phys. Org. Chem.* **1963**, *1*, 109.

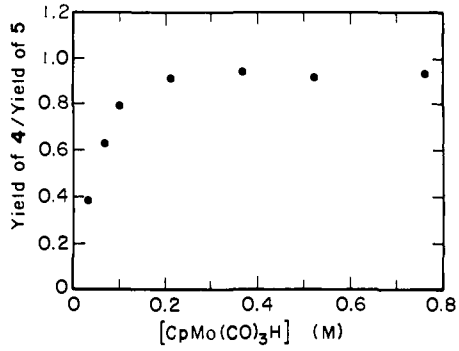

Figure 5. Plot of the yield ratio of **4**/**5** vs. $CpMo(CO)_3H$ in the reaction of **1** with varying concentrations of $CpMo(CO)_3H$ at 20 °C.

effects are inverse but quite small, typically 0.97 per deuterium. We can therefore estimate that the secondary contribution to the effect we have measured is very probably no larger than 0.90, and making this correction the primary isotope effect for addition of the metal hydride (deuteride) to the vinylidene carbon is 0.70.

Dependence of the Product Distribution on Hydride Concentration: Evidence for Caged Radical Pairs. As an approach to confirming the mechanism in Scheme III, the reaction of **1** with $CpMo(CO)_3H$ was run in the presence of 9,10-dihydroanthracene (DHA) or 1,4-cyclohexadiene, both good hydrogen atom donors, in the hope of trapping intermediate A to produce **4**. Addition of either of these trapping agents did in fact result in the formation of substantial amounts of **4** (up to 50%) and reduced yields of **5**. In control experiments, adding DHA or 1,4-cyclohexadiene to **1** alone did not give any **4**. Reproducibility of the yields of **4** in the $CpMo(CO)_3H$ reaction was poor, however.

The problem of trapping intermediate A reproducibly was resolved by utilizing one of the reagents, $CpMo(CO)_3H$, as the hydrogen atom donor. As mentioned earlier, when the reaction of **1** + $CpMo(CO)_3H$ was not carried out under high dilution, hydrogenated alkylidene **4** was observed as a side product. This hydrogenated product can be accounted for by assuming that after the bridged radical C escapes the cage A (Scheme III), it is scavenged by donation of a hydrogen atom from a second molecule of hydride, leading to **4**. This mechanism predicts a very specific dependence of the product distribution on the concentration of hydride, analogous to that observed in organic radical reactions which proceed through cages: increasing the hydride concentration should increase the ratio of hydrogenated product **4** to cluster **5**, until all the free (escaped) radicals are being scavenged. At that point, further increases in the hydride concentration should no longer change the ratio.[16] As shown in Figure 5, this is exactly the behavior observed in our system. The ratio increases with $[CpMo(CO)_3H]$ at low concentrations of hydride, and this dependence does level off at high $[CpMo(CO)_3H]$. The yield of **4** never exceeds 50%, which indicates that after solvent cage A is initially formed, roughly half of the radical pairs escape, and half collapse to form the cluster.

Viscosity Effects. Further evidence for the existence of a solvent cage was provided by studying the reaction of **1** with $CpMo(CO)_3H$ in solvents of different viscosities. It is known that the rate of escape from a cage by a radical pair decreases as the solvent becomes more viscous.[17] In the mechanism shown in Scheme III, increasing solvent viscosity should result in a decrease in k_{esc} relative to $k_{collapse}$, leading to a decrease in the yield of hydrogenation product **4** relative to cluster **5**. The experiments were run at room temperature using benzene, *p*-xylene, *o*-xylene, and Nujol as solvents and identical concentrations of $CpMo(CO)_3H$ (0.2 M) and **1** (0.066 M) for each run. The isomeric xylene solvents were chosen due to the fact that they are structurally and chemically similar, yet they have significantly different viscosities. The results are summarized in Table V. In benzene and *p*-xylene, solvents of similar viscosity, the relative yields of **4** and **5** were almost identical. In *o*-xylene, a significant increase in the yield of cluster **5** was observed, and in Nujol cluster was obtained almost exclusively.

Table V. Effect of Solvent Viscosity on the Relative Yields of Cluster **5** and Hydrogenated Product **4** in the Reaction of Vinylidene **1** with $Cp(CO)_3MoH$[a]

solvent	viscosity,[b] cp	% yield [**4**]	% yield [**5**]	[**4**]/[**5**]
benzene	0.652	36	40	0.90
p-xylene	0.648	44	46	0.96
o-xylene	0.810	22	61	0.36
Nujol	>200	4.8	77	0.06

[a] [**1**] = 3.3×10^{-2} M; $[Cp(CO)_3MoH]$ = 0.20 M. [b] Taken from "Handbook of Chemistry and Physics", 51st ed.; The Chemical Rubber Co.: Cleveland, OH, 1970–71, F37–40.

Scheme V

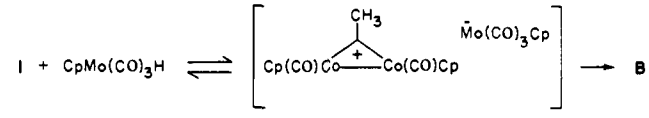

Scheme VI

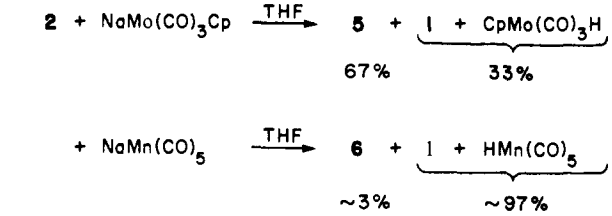

Behavior of the Caged Radicals: An Extremely Rapid Hydrogen Transfer. There is one consequence of the radical cage mechanism which remains a bit puzzling. The trapping experiments described above indicate that in benzene k_{esc} and $k_{collapse}$ (Scheme III) are approximately equal. It is surprising that the rate constant k_{-1} for the back reaction, which results in the H/D exchange described earlier, is observed to be so much greater (exchange occurs at least 100 times faster than either cluster formation or hydrogenation). Bimolecular reactions which are "diffusion controlled", i.e., experience only the barrier to diffusion through solvent in order to react, typically occur with rate constants in the range of 10^9 M^{-1} s^{-1}. Since diffusion of radicals *out* of a cage does not suffer similar entropic restrictions, it must occur with rates near 10^{11}–10^{12} s^{-1}. Thus, the substantially more rapid rate of exchange requires that k_{-1} must be of the order of 10^{13}–10^{14} s^{-1}, which is extremely rapid—probably close to the rate of a molecular vibration.[18]

Caged organic radicals, such as alkyl radicals, also undergo reactions which involve hydrogen atom transfer to generate a new C—H bond and a C=C double bond ("disproportionation"), escape from the cage, or combination to give a new, longer chain alkane. In such organic cages it is generally found that k_{esc}, k_{comb}, and k_{disp} have much more comparable values than those observed for the organometallic cage A in Scheme VI. However, such caged alkyl radical pairs are often generated from precursors such as azo compounds or peresters. Thus they are born initially with

(16) This method for determining the extent of cage escape by a radical pair has long been in use. See: Hammond, G. S.; Sen, J. N.; Boozer, C. E. *J. Am. Chem. Soc.* **1955**, *77*, 3244.

(17) Koenig, T.; Fischer, H. In "Free Radicals"; Kochi, J. K, Ed.; Wiley: New York, 1973; Vol. I, 170.

(18) Another way to account for the large k_{-1}/k_{esc} ratio is to assume that k_{esc} is unusually slow, perhaps because of size or steric effects of the radicals in cage A. However, changes in size much larger than those in consideration here are apparently required to affect diffusion rates significantly. For example, most radical termination rates, which are commonly thought to be "diffusion controlled", vary over quite a small range for typical organic radicals, despite significant differences in size and steric hindrance (e.g., in cyclohexane at 25 °C, k_{methyl} = 8.9, $k_{neopentyl}$ = 4.0, k_{benzyl} = 4.0, $k_{t\text{-}Bu}$ = 2.1, k_{cumyl} = 16 M^{-1} s^{-1}). Slower diffusion is observed only for radicals of substantially larger size—for example, in polymerization reactions it is estimated that the chain length of an organic radical must be 100 in order to reduce the rate of its radical–radical reactions by a factor of 5. See: Ingold, K. U. In "Free Radicals"; Kochi, J. K.; Eds.; Wiley-Interscience: New York, 1973; Vol. 1, pp 40–57 and references cited therein.

at least one gas molecule located in between the two radicals; i.e., the radicals are generated with a significantly longer distance between the centers, and perhaps also in a relative orientation inappropriate for hydrogen transfer. This may well be responsible for slowing the rate of hydrogen transfer relative to that which would prevail if the radicals were born with a smaller intermolecular separation.

Organic radical reactions do exist in which cages can be generated without intervening gas molecules. Singer and his coworkers found that caged radicals of similar structure generated with and without intervening gas molecules showed somewhat higher cage reaction/cage escape ratios and significantly higher recombination/racemization ratios when the gas molecule was absent.[19] Even more closely associated radical pairs are apparently generated in the rearrangement of nitrogen ylides to amines and α-alkoxy carbanions to alkoxides (the so-called Stevens and Wittig rearrangements).[20] These reactions proceed with variable—but in some cases very small—amounts of cage escape products. They can also proceed with high degrees of retention of configuration in the recombination products when optically active starting materials are used. However, substituent effects and the observation of CIDNP provide strong evidence that these reactions proceed via the formation and recombination of caged radicals. In these systems, k_{comb}/k_{esc} may well be as large as the k_{-1}/k_{esc} ratios observed in our Co_2/Mo study.

The above results demonstrate that at least in some cases, organic radicals generated with appropriate proximity and orientation can recombine at rates substantially faster than they escape the cage. The organometallic cage A in Scheme III should have properties ideal for very rapid hydrogen transfer to regenerate vinylidene and metal hydride. The general orientation of the two radicals will be nearly perfect, since they are formed in a reaction which is the exact reverse of k_{-1}. Once they are generated, only a partial rotation of the new methyl group must occur before back transfer of the hydrogen atom is possible, and so an absolute minimum of molecular motion is required. Finally, the reaction involves transfer of a very light atom, and may be accelerated by tunnelling.

In order to account completely for our results, one must also assume that the barrier associated with $k_{collapse}$ is comparable to that associated with escape from the cage, despite the proximity of the two radicals. It is not difficult to believe such a barrier exists, since the two radicals are very hindered, and $k_{collapse}$ may require substantial distortion of the ligands attached to the metal centers. Thus it seems reasonable that hydrogen/deuterium exchange in this system is very rapid compared to both of the other reactions experienced by the caged radicals.[21]

Consideration of Possible Alternative Mechanisms. Although all of the evidence given above strongly supports the nonchain radical mechanism in Scheme III, it is worthwhile at this point to examine alternative mechanisms to see if any of these also fit the data. Since $CpMo(CO)_3H$ is an acid of moderate strength (pK_a = 13.9 in acetonitrile),[22] it seems possible that it may transfer a proton to **1** to give an intermediate ion pair which could then give B (Scheme V). In order to test this mechanism, we treated ethylidyne salt **2** with $NaMo(CO)_3Cp$ in THF. These two complexes reacted instantly to give cluster **5** as well as the products of proton transfer **1** and $CpMo(CO)_3H$ (Scheme VI). Reaction of **2** with $NaMn(CO)_5$ afforded proton-transfer products almost exclusively, along with a very small amount of cluster **6**. The fact that both vinylidene and cluster complex are formed in this reaction is consistent with the possibility that ions are intermediates in the vinylidene/hydride reaction. The ratio of these two products is substantially different from that which would be predicted by the $k_{-1}/k_{collapse}$ ratio determined in the latter reaction; however, we have made a case above that such ratios may be very sensitive to the precise location of the two species in the radical or ion pair. We therefore cannot rule out ionic intermediates on the basis of these results.

Table VI. Rate Date for Reaction of Molybdenum Hydrides $Cp(CO)_2(L)MoH$ with Vinylidene **1**[a]

L	k, M^{-1} s^{-1}
CO	$(1.3 \pm 0.1) \times 10^{-2}$
PMe_3	$(6.4 \pm 0.1) \times 10^{-2}$
PPh_3	$(8.0 \pm 0.1) \times 10^{-3}$

[a] In C_6H_6, 60 °C. Pseudo-first-order conditions with [**1**] = 7×10^{-4} M.

However, further experiments provided much stronger evidence against ionic intermediates. The influence of solvent polarity was examined by carrying out the reaction of **1** with $CpMo(CO)_3H$ in THF, a more polar medium than benzene. The THF reaction is much less clean than the reaction in benzene. Although quantitative rate data could not be obtained due to the appearance of significant amounts of paramagnetic and insoluble materials, it is clear that the major products and rate of reaction are very similar in the two solvents. This is inconsistent with a proton-transfer mechanism, since the ionic intermediates produced would be better stabilized by THF, and the rate should be faster in that solvent; a radical pathway would not be expected to show a large dependence on solvent polarity.

Most convincing evidence against an ionic pathway was provided by examining the rate of reaction of the phosphine-substituted hydrides $Cp(CO)_2(PR_3)MoH$ (R = Me, Ph) with **1**. Kinetics performed on these reactions in benzene were well-behaved and showed that the bimolecular rate constants for these two reactions are quite similar to k_H obtained in the parent system (Table VI). There is now substantial evidence that the pK_a of a transition metal hydride, as well as its rate of proton transfer to basic acceptors, is reduced by several orders of magnitude upon substitution of a phosphine for a CO ligand on the metal.[22,23] This effect is attributable to CO's better back-bonding ability, which is critical to the stabilization of the conjugate metal base. Because of this, it is extremely improbable that $Cp(CO)_3MoH$, $Cp(CO)_2(PPh_3)MoH$, and $Cp(CO)_2(PMe_3)MoH$ would transfer their metal-bound protons to vinylidene **1** at comparable rates.

Unfortunately, it is much more difficult to predict the relative rate of a hydrogen *atom* transfer by $Cp(CO)_3MoH$ or $Cp(CO)_2(PR_3)MoH$ to **1**—the necessary first step in our proposed radical mechanism—since data on the M–H bond dissociation energies are not available. One might expect the phosphine-substituted hydrides to be more stable than the tricarbonyl hydride due to electronic factors, but the steric demands of the phosphine ligands and the effect of PR_3 on the stability of $Cp(CO)_2(PR_3)Mo\cdot$ might also favor the loss of H· relative to the tricarbonyl analogue. If this is the case, it is possible that phosphine substitution might have a small effect on the M–H bond dissociation energy. Thus, known acidity data allow us to rule out the ionic mechanism, but the lack of analogous bond energy data prevent us from making a clear evaluation of the radical mechanism. However, in light of the weight of our other data, discussed above, in support of hydrogen atom transfer, we predict that the Mo–H bond dissociation energies will turn out to be quite insensitive to phosphine substitution in this system.

Another mechanistic possibility which should be considered is a classical alkene-insertion pathway. In this alternative, loss of CO would presumably have to occur to generate a coordinatively

(19) Lee, K.-W.; Horowitz, N.; Ware, J.; Singer, L. A. *J. Am. Chem. Soc.* **1977**, *99*, 2622.

(20) See, for example: Ollis, W. D.; Rey, M.; Sutherland, I. O.; Closs, G. L. *J. Chem. Soc., Chem. Commun.* **1975**, 543 and references cited there.

(21) It is of course possible that the exchange occurs via a mechanism independent of the radical pathway. However, alternate mechanisms, such as those which will be described shortly, seem unlikely: the exchange is equally rapid whether $CpMo(CO)_3D$ or the less acidic $CpMo(CO)_2(PMe_3)D$ is used, ruling out an ionic mechanism; also it is unaffected by added CO, providing evidence against a dissociative pathway.

(22) E.g., at 25 °C in CH_3CN solvent: for $(CO)_4CoH$, pK_a = 8.5, k_{H^+} (rate of proton transfer to aniline) ca. 7×10^7 M^{-1} s^{-1}; $(CO)_3(PPh_3)CoH$, pK_a = 15.5, $k_{H^+} = 3.3 \times 10^4$ M^{-1} s^{-1}; $Cp(CO)_3WH$, pK_a = 16.1, $k_{H^+} = 2.5 \times 10^2$ M^{-1} s^{-1}; $Cp(CO)_2(PMe_3)WH$, pK_a = 27.3, $k_{H^+} < 10^{-3}$ M^{-1} s^{-1}. Jordan, R. F.; Norton, J. R. *J. Am. Chem. Soc.* **1982**, *104*, 1255. Norton, J., private communication.

(23) Shriver, D. F. *Acc. Chem. Res.* **1970**, *3*, 231.

unsaturated molybdenum center, followed by coordination of the vinylidene C=C bond to the metal. Insertion of the double bond into the Mo–H bond would give an intermediate similar to B in Scheme VI, capable of leading to cluster. Since recoordination of CO to unsaturated molybdenum would undoubtedly be a rapid reaction, the initial CO dissociation step would have to be reversible, and this mechanism predicts that added CO should produce a strong rate inhibition. This is not observed: no significant rate inhibition occurs upon addition of free CO to the reaction of **1** with $CpMo(CO)_3H$ ($k_{obsd} = 3.9 \times 10^{-4}$ s^{-1} without CO, $k_{obsd} = 3.5 \times 10^{-4}$ s^{-1} under 2 atm CO). Qualitative measurements also showed no rate inhibition by PPh_3 in the $CpMo(CO)_2(PPh_3)H$ reaction. Additionally, the observed dependence of the product distribution on molybdenum hydride concentration would not be consistent with this mechanism. A concerted alternative to the olefin insertion mechanism, in which Mo–H adds across the vinylidene double bond without prior loss of CO from the metal center, would also be inconsistent with the effect of hydride concentration on the ratio of cluster to hydrogenation product.

Conclusion

The chemistry of the carbon–carbon double bond in vinylidene complex **1** is strongly influenced by the attached dicobalt functionality. Hydrogenation of the double bond is facile and requires no added catalyst, occurring upon moderate heating with H_2 in solution. Protonation by a strong acid yields an isolable salt, **2**, showing that the dicobalt system is capable of stabilizing a positive charge on a bridging carbon, as has been observed in other dinuclear vinylidene complexes.

We have also obtained strong evidence that in the reaction with molybdenum hydrides, the terminal vinylidene carbon accepts a hydrogen atom to produce an intermediate radical species which then reacts further to give either hydrogenation or heteronuclear cluster. To our knowledge, this is the first demonstration that a dimetal functionality is capable of stablilizing an attached radical center in much the same way that it stabilizes a cationic carbon center. Our results also reinforce the idea, established earlier by Halpern,[13] that cage effects very similar to those observed in many organic systems can also play an important role in organotransition metal reactions—including cluster formation processes. As a result of this radical mechanism, metal hydrides with weak M–H bonds give simple hydrogenation of the vinylidene double bond, whereas those with strong M–H bonds do not readily transfer a hydrogen atom to give the required radical intermediate. Thus the cluster synthesis can only be observed with hydrides having bond strengths which lie within a certain, very specific range. They must be weak enough to allow the initial hydrogen transfer, but strong enough to retard the subsequent hydrogen transfer to the dicobalt radical, so that even after escape from its initial cage, the radical will have a long enough lifetime to combine with the molybdenum radical to regenerate the cage capable of leading to cluster. Although this limits the scope of the reaction studied in the present case, our understanding of this system makes it substantially more predictable. It is our hope that further mechanistic studies will extend this predictability to nonradical cluster-forming reactions.

Experimental Section

General. All manipulations of oxygen- or water-sensitive materials were carried out in a Vacuum Atmospheres 553-2 drybox with attached M6-40-1H Dritrain, or by using standard Schlenk or vacuum line techniques. ^{1}H NMR spectra were recorded either on the 180-MHz, 200-MHz, 250-MHz, or 300-MHz spectrometers constructed by Rudi Nunlist at the University of California at Berkeley (UCB) NMR facility. ^{13}C NMR spectra were recorded at 63.2 MHz on the UCB-250 or at 75.4 MHz on the BVX-300 spectrometer. NMR data are reported in parts per million relative to tetramethylsilane internal standard.

IR spectra were obtained on a Perkin-Elmer Model 283 infrared spectrophotometer or on a Perkin-Elmer Model 1550 FT-IR spectrophotometer using potassium bromide solution cells (0.1-mm path length) or potassium bromide ground pellets. UV/Vis spectra were recorded on a Hewlett-Packard Model 8450A spectrophotometer equipped with a Model 89100A Temperature Control Accessory. Mass spectroscopic (MS) analyses were obtained on an AEI MS-1 spectrometer interfaced with a Finnigan 2300 data system. The fast atom bombardment (FAB) spectrum was obtained on a Kratos MS-50 spectrometer. Elemental analyses were obtained from UC Berkeley analytical facility. Melting points were recorded on a Thomas-Hoover capillary melting point apparatus and are uncorrected.

Unless otherwise specified, reagents were used as received from commercial suppliers. $CpCo(CO)_2$ was prepared from $Co_2(CO)_8$ by the method of Rausch and Genetti.[24] $Na[Cp_2Co_2(CO)_2]$ was prepared by the published procedure,[25] and the material used was a crude mixture containing approximately 70% of the radical anion by weight.

$CpM(CO)_3H$ (M = Cr, Mo, W) and $CpMo(CO)_3D$ were synthesized according to published procedures and exhibited satisfactory spectroscopic and physical properties.[26] $CpCr(CO)_3H$ was sublimed at 45 °C/1 torr immediately prior to use. $CpMo(CO)_3H$ was sublimed at 60 °C/1 torr and stored in the dark at −40 °C. $(CO)_5MnH$ was also synthesized according to published procedures[27] and was stored under vacuum in the dark.

Dichloromethane, acetonitrile, and pentane were dried by vacuum transfer from calcium hydride. Ethanol was vacuum transferred from magnesium ethoxide. Hexane (UV grade, alkene free) was distilled under nitrogen from *n*-butyllithium. Nujol was dried over freshly cut sodium and stored under nitrogen. All other solvents were dried with sodium–benzophenone ketyl and distilled under nitrogen except for *o*- and *p*-xylene, and tetraglyme which were distilled under vacuum. Deuterated solvents for use in NMR experiments were treated as their protiated analogues and degassed via three successive freeze–pump–thaw cycles.

1,1-Dibromoethylene.[9] Potassium acetate (3.69 g, 0.0376 mol), potassium carbonate (5.18 g, 0.0375 mol), and dry ethanol (30 mL) were placed in a 100-mL, 3-neck, roundbottom flask. A dropping funnel containing 1,1,2-tribromoethane[28] (10.0 g, 0.0375 mol) was connected to the flask. A nitrogen inlet valve was connected to another neck of the flask, and a Dean–Stark distillation apparatus was attached to the remaining neck. The entire system was thoroughly purged with nitrogen before the addition, as the product is quite oxygen sensitive. The system was heated to reflux, and once ethanol began to collect in the Dean–Stark trap, the 1,1,2-tribromoethane was added as rapidly as possible. Distillation was continued until only a solid salt cake remained in the flask. The distillate was added under a stream of nitrogen to 50 mL of nitrogen-saturated water. A clear oily layer was separated, dried over calcium chloride, and stored in the drybox at −40 °C. ^{1}H NMR of this material showed a single peak at δ 5.67 (C_6D_6); yield, 3.54 g (54%). Because of its sensitivity, it was used in the following preparation without further purification.

(μ-Vinylidene)bis[(η^5-cyclopentadienyl)carbonylcobalt] (1). 1,1-Dibromomethane (4.00 g, 21.4 mmol) was added all at once to a stirred slurry of crude $Na[Cp_2Co_2(CO)_2]$ (8.12 g, 17.4 mmol) in THF (100 mL). An immediate color change to blue green was accompanied by the appearance of new IR absorbances at 1796 and 2020 cm^{-1} (due to neutral dimer $[CpCo(CO)]_2$[25] and $CpCo(CO)_2$[24], respectively) and of a very strong absorbance at 1960 cm^{-1}. The reaction was complete within 5 min, at which point hexane (40 mL) was added and the precipitated NaBr was removed by filtration. The volatile materials were removed by vacuum transfer and the brown residue was chromatographed in the drybox on neutral alumina II eluting with hexane/benzene (3:1) to yield a deep red solution of pure **1**. Recrystallization from hexane yielded 1.39 g of large black polyhedral crystals (48% of the theoretical yield, assuming the reaction produces 1 equiv of $[CpCo(CO)]_2$): mp 73–74 °C; ^{1}H NMR (C_6D_6) δ 6.10 (s, 1 H), 4.64 (s, 5 H); ^{13}C NMR (C_6D_6) δ 247.8 (μ-C=CH_2), 206.8 (CO), 125.7 (μ-C=CH_2), 87.5 (C_5H_5); MS (15 eV), *m/e* 330 (M^+); IR (KBr pellet) 1960 (s). Anal. Calcd for $C_{14}H_{12}Co_2O_2$: C, 50.94; H, 3.66; Co, 35.70. Found: C, 51.07; H, 3.81; Co, 35.2.

Crystal and Molecular Structure Determination of 1. A fragment cleaved from a large crystal was mounted in a capillary in air. The capillary was then flushed with dry nitrogen and flame sealed. Table I lists the final cell parameters and specific data collection parameters. The full details of the study were included as supplementary material in the preliminary communication on this work.[7]

(μ-Ethylidyne)bis[(η^5-cyclopentadienyl)carbonylcobalt] Tetrafluoroborate (2). At ambient temperature, HBF_4·OEt_2 (100 mg, 0.618 mmol) was added dropwise to a stirred solution of **1** (200 mg, 0.606 mmol) in diethyl ether (20 mL). Within 30 s the color of the solution changed

(24) Rausch, M. D.; Genetti, R. A. *J. Org. Chem.* **1970**, *11*, 3888.
(25) Schore, N. E.; Ilenda, C. S.; Bergman, R. G. *J. Am. Chem. Soc.* **1977**, *99*, 1781.
(26) Davison, A.; McCleverty, J. A.; Wilkinson, G. *J. Chem. Soc.* **1963**, 1133.
(27) King, R. B.; Stone, F. G. A. *Inorg. Synth.* **1963**, *7*, 196.
(28) Prepared in 95% yield by the addition of excess vinyl bromide to a CCl_4 solution of Br_2 at room temperature.

from deep red to a very faint blue as a black solid precipitated. The latter was isolated by filtration to yield 241 mg of analytically pure **2** (95% yield). ^{1}H NMR (CD_2Cl_2 "100% D", −30 °C) δ 5.43 (s, 10 H), 4.37 (s, 3 H); MS (FAB, thioglycerol), m/e 418 (M^+), 390 (M^+ − CO), 362 (M^+ − 2CO). IR (CH_2Cl_2) 2060 (s), 2033 (s), 1884 (br, s). Anal. Calcd for $C_{14}H_{13}BCo_2F_4O_2$: C, 40.24; H, 3.14; Co, 28.20. Found: C, 40.11; H, 3.10; Co 28.1.

(μ_3-Ethylidyne)bis(carbonyl)tris[(η^5-cyclopentadienyl)cobalt] Tetrafluoroborate (3). A solution of 322 mg of **2** (772 mmol) in methylene chloride (30 mL) was allowed to stir under N_2 at room temperature for 1 h, during which time the color turned from deep blue to green. The mixture was filtered and 20 mL of THF was added to the filtrate. The solution was then allowed to stand uncovered until approximately all but 10 mL of solvent had evaporated. The resulting crystals were isolated by filtration and washed several times with THF to give 230 mg of shiny black needles of **3** (82% yield based on cobalt). ^{1}H NMR (CD_3CN) δ 5.66 (s, 3 H), 5.19 (s, 15 H); $^{13}C\{^1H\}$ NMR (CD_3CN) δ 371.3 (vw, br) (C-CH_3), 229.4 (CO), 92.8 (C_5H_5), 60.1 (CH_3); MS (FAB, thioglycerol), m/e 455 ($M^+ - BF_4$); IR (CH_3CN) 1910 (s), 1870 (s). Anal. Calcd for $C_{19}H_{18}BCo_3F_4O_2$: C, 42.11; H, 3.35. Found: C, 42.22; H, 3.45.

(μ-Ethylidene)bis[(η^5-cyclopentadienyl)carbonylcobalt] (4). A suspension of $NaBH_4$ (9 mg, 0.24 mmol) in THF (3 mL) was added all at once to a stirred suspension of **2** (74 mg, 0.18 mmol) in THF (2 mL) at ambient temperature. The solution turned dark red almost immediately. The mixture was stirred for 15 min, the solvent removed in vacuo, and the residue chromatographed in the drybox on neutral alumina II eluting with hexane. The first band to elute, a red fraction, was collected and solvent was removed by vacuum transfer. The residue was sublimed at 60 °C/0.1 torr to yield 20 mg (34% yield) of red microcrystalline **4**: mp 63–64 °C; ^{1}H NMR (C_6D_6) δ 8.28 (q, 1 H, J = 7.4 Hz), 4.61 (s, 10 H), 2.35 (d, 3 H, J = 7.4 Hz); MS (15 eV), m/e 332 (M^+); IR (C_6H_6) 1951 (s) cm^{-1}. Anal. Calcd for $C_{14}H_{14}Co_2O_2$: C, 50.63; H, 4.25. Found: C, 50.79; H, 4.40.

Reaction of 1 with H_2. An NMR tube was charged with 9.0 mg of **1** (0.027 mmol) and 3.7 mg of ferrocene internal standard (0.020 mmol) and benzene-d_6 (0.6 mL) was vacuum transferred in. With the tube kept at −196 °C and open to a vacuum line, H_2 was admitted to the system until the pressure reached 600 torr. The tube was then sealed just above the surface of the liquid nitrogen in order to maximize the H_2 pressure within the tube (approximately 3.0 atm at room temperature). The initial NMR spectrum showed resonances due only to **1** and dissolved H_2 (δ 4.46). The tube was placed in a 60 °C bath and the reaction was monitored by NMR. Resonances due to **4** appeared after 1 h and continued to increase in intensity relative to the ferrocene resonance until reaching a maximum after 10 h corresponding to 43% yield (80% conversion of **1**). Further heating resulted in complete disappearance of **1**, but also to a decrease in intensity of signals due to **4**, with concurrent appearance of resonances at δ 5.24 (ethylene) and 0.79 (ethane).

(μ_3-Ethylidyne)(μ_2-carbonyl)bis[(η^5-cyclopentadienyl)cobalt](η^5-cyclopentadienyl)dicarbonylmolydenum (5). In the drybox, a 100-mL round-bottom flask was charged with **1** (33.4 mg, 0.101 mmol), $CpMo(CO)_3H$ (25.5 mg, 0.104 mmol), and benzene (40 mL). The flask was fitted with a condenser and a vacuum stopcock and removed from the box. The solution was heated in an oil bath at 64 °C for 12 h under nitrogen as the color turned from deep red to dark green. Solvent was then removed by vacuum transfer and the residue was chromatographed in the drybox on silica eluting with benzene. A dark green band was collected. Recrystallization from toluene/pentane yielded 40 mg of **5** (76% yield) as a dark green crystalline powder: mp, no detectable melting or decomposition below 220 °C; ^{1}H NMR (C_6D_6) δ 4.74 (s, 5 H), 4.69 (s, 3 H), 4.44 (s, 10 H); ^{13}C NMR (CD_2Cl_2, gated spectrum) δ 341.2 (s, μ-CCH_3), 238.8 (s, CO), 92.4 (d, C_5H_5, J = 12.8 Hz), 89.7 (d, C_5H_5, J = 11.6 Hz), 55.3 (q, μ-CCH_3, J = 13.1 Hz, one line obscured by solvent resonances), 129.0 (very small resonance,not assignable); MS (15 eV), m/e 518, 519, 520, 521, 522, 524 (M^+ for each of the naturally occurring isotopes of Mo); IR (Nujol mull) 1874 (s), 1830 (s), 1778 (s) cm^{-1}; IR (C_6H_6) 1966 (s), 1905 (s), 1837 (s), 1816 (s), 1793 (s), 1745 (s) cm^{-1}. Anal. Calcd for $C_{20}H_{18}Co_2MoO_3$: C, 46.18; H, 3.49. Found: C, 46.13; H, 3.60.

Crystal and Molecular Structure Determination of 5. Large shiny black crystals of the compound were obtained by slow crystallization from hexane/benzene by vapor diffusion at room temperature. Fragments cleaved from some of these crystals were mounted in capillaries in air, the capillaries flushed with dry nitrogen, and then flame sealed. Preliminary precession photographs indicated monoclinic Laue symmetry but also showed severe twinning. Carefully selected samples were examined until one untwinned specimen was found. Precession photos on this sample confirmed the Laue symmetry and yielded preliminary cell dimensions. Systematic absences were consistent only with space group $P2_1/c$.

The crystal used for data collection was then transferred to our Enraf-Nonius CAD-4 diffractometer; the structure analysis was carried out by using procedures similar to those described in detail in an earlier study.[29] The final cell parameters and specific data collection parameters are given in Table I. The 2671 raw intensity data were converted to structure factor amplitudes and their esds.[29] No correction for crystal decomposition was necessary. Inspection of the azimuthal scan data showed a variation I_{min}/I_{max} = 0.78 for the average curve. An absorption correction based on the measured shape and size of the crystal and a 10 × 16 × 6 Gaussian grid of internal points was applied to the data following solution and isotropic refinement of the structure (T_{max} = 0.765, T_{min} = 0.582). Removal of systematically absent and redundant data left 2304 unique data.

The structure was solved by Patterson methods and refined via standard least-squares and Fourier techniques. In a difference Fourier map calculated following refinement of all non-hydrogen atoms with anisotropic thermal parameters, peaks corresponding to the expected positions of all of the hydrogen atoms were found. Hydrogens were included in the structure factor calculations in their expected positions based on idealized bonding geometry but were not refined in least square. They were assigned isotropic thermal parameters of either 5.0 or 6.0 Å^2 depending on the B_{eqv} of the carbon to which they were attached.

The final residuals for 235 variables refined against the 2059 data for which $F^2 > 3\sigma(F^2)$ were R = 1.77%, R_w = 2.74% and GOF = 1.885. The R value for all 2304 data was 2.32%. The analytical and statistical forms used were the same as described earlier.[29] Inspection of the residuals ordered in ranges of $(\sin\theta)/\lambda$, $|F_o|$, and parity and value of the individual indexes showed no unusual features or trends. There was no evidence of secondary extinction in the low-angle, high-intensity data. The largest peak in the final difference Fourier map had an electron density of −0.37 e$^-$/Å$^+$ and was located near the Mo atom. The positional and thermal parameters of the refined atoms, the positions of the hydrogen atoms, and a listing of the values of F_o and F_c are available as supplementary material.

Reaction of 1 with $CpMo(CO)_2(PR_3)H$ (R = Ph, Me). The reactions were run in a similar manner as described above for the reaction of **1** with $CpMo(CO)_3H$, but on small scale (e.g., 15 mg of **1**). In both cases, **5** was isolated by chromatography on silica and the amount isolated quantified by NMR using ferrocene as an internal standard. Yield: 81% (R = Ph), 80% (R = Me).

Reaction of 1 with $CpCr(CO)_3H$. An NMR tube was charged with **1** (8.5 mg, 0.026 mmol) and $CpCr(CO)_3H$ (5 mg, 0.025 mmol). Benzene (0.9 mL) was vacuum transferred in and the tube sealed. An initial NMR spectrum at −70 °C showed the presence of only starting materials. Warming the tube to room temperature in the NMR probe resulted in the complete disappearance of resonances due to $CpCr(CO)_3H$ and the appearance of those due only to **4**, $CpCo(CO)_2$, and $[CpCo(CO)]_n$ clusters. The yield of **4** was approximately 50% by ^{1}H NMR based on **1**.

Reaction of 1 with $CpW(CO)_3H$. An NMR tube was charged with **1** (22.6 mg, 0.068 mmol) and $CpW(CO)_3H$ (24.2 mg, 0.072 mmol). Benzene (1 mL) was vacuum transferred in and the tube sealed. The initial spectrum, taken at room temperature, showed only starting materials, so the tube was heated to 60 °C and the reaction monitored by NMR. Resonances due only to decomposition products of **1** ($CpCo(CO)_2$ and cobalt tri- and tetranuclear clusters) and of $CpW(CO)_3H$ (mostly $[CpW(CO)_3]_2$) appeared after heating for 48 h. No identifiable Co–W clusters could be detected.

(μ_3-Ethylidyne)bis[(η^5-cyclopentadienyl)cobalt]bis(μ-carbonyl) Tricarbonylmanganese (6). Into a 250-mL Schlenk flask were placed **1** (120 mg, 0.364 mmol) and C_6H_6 (100 mL). The solution was heated to 60 °C under a flow of N_2 with stirring as a solution of $(CO)_5MnH$ (93 mg, 0.474 mmol) in C_6H_6 (30 mL) was added over 44 h via a 50-mL syringe set in a syringe pump. When addition was complete, volatile materials were removed in vacuo and the black residue was chromatographed on silica eluting with hexane/benzene (1:1) to yield a single dark green fraction. Recrystallization from pentane afforded 150 mg of 6 (88% yield): mp, no detectable melting or decomposition below 200 °C; ^{1}H NMR (C_6D_6) δ 4.76 (s, 10 H), 4.26 (s, 3 H); ^{13}C NMR (C_6D_6) δ 344.4 (μ-CCH_3), 229.4 (CO), 89.8 (C_5H_5), 52.9 (CH_3); IR (KBr pellet) 2030 (s), 2020 (sh), 1980 (s), 1965 (s), 1949 (m), 1938 (m), 1822 (s), 1796 (s); IR (C_6H_6) 2020 (s), 1962 (s, br), 1890 (s, br), 1769 (w), 1677 (w); MS (15 eV), m/e 470 (M^+). Anal. Calcd for $C_{17}H_{13}Co_2MnO_5$: C, 43.44; H, 2.79. Found: C, 43.09; H, 2.84.

Crystal and Molecular Structure Determination of 6. Large clusters of overlapping tablet-shaped crystals of the compound were obtained by slow crystallization from toluene/pentane. Fragments cleaved from some

(29) Hersh, W. H.; Hollander, F. J.; Bergman, R. G. *J. Am. Chem. Soc.* **1983**, *105*, 5831.

of these crystals were mounted as for **5**. Preliminary precession photographs indicated triclinic Laue symmetry and yielded preliminary cell dimensions. The crystal used for data collection was then transferred to our diffractometer and examined by using procedures described earlier.[29] The final cell parameters and specific data collection parameters are given in Table I.

The 4503 unique raw intensity data were converted to structure factor amplitudes and their esds. No correction for crystal decomposition was necessary. Inspection of the azimuthal scan data showed a variation $I_{min}/I_{max} = 0.92$ for the average curve. An empirical correction for absorption, based on the azimuthal scan data, was applied to the intensities after solution and partial refinement of the structure.

The structure was solved by using MULTAN 11/82 and Patterson methods and refined via standard least-squares and Fourier techniques. The assumption that the space group was $P\bar{1}$ was confirmed by the successful solution and refinement of the structure. In a difference Fourier map calculated following refinement of all non-hydrogen atoms with anisotropic thermal parameters, peaks corresponding to the expected positions of most of the hydrogen atoms were found. Hydrogens were included in the structure factor calculations in their expected positions based on idealized geometry but were not refined in least squares. They were assigned isotropic thermal parameters 1–2 Å^2 larger than the equivalent B_{iso} of the atom to which they were bonded. In the final cycles of least squares an isotropic extinction coefficient was refined.[30]

The final residuals for 452 variables refined against the 3579 data for which $F^2 > 3\sigma(F^2)$ were $R = 2.32\%$, $R_w = 2.87\%$, and GOF = 1.735. The R value for all 4503 data was 4.07%. The analytical and statistical forms used were the same as those described for **5**. Inspection of the residues ordered in ranges of $(\sin\theta)/\lambda$, $|F_o|$, and parity and value of the individual indexes showed no unusual features or trends. The largest peak in the final difference Fourier map had an electron density of 0.34 e$^-$/Å$^+$ and was located near Co12.

The positional and thermal parameters of the refined atoms, the positions of the hydrogen atoms, and a listing of the values of F_o and F_c are available as supplementary material.

UV–Visible Kinetics. A stock solution of **1** in C_6H_6 ([**1**] = 1.4 10^{-3} M) was used in all the measurements. In each run, a known amount of the appropriate molybdenum hydride or deuteride reagent was dissolved in 1.00 mL of C_6H_6 and added to 1.00 mL of the stock solution of **1**. The solution thus obtained, 0.7×10^{-3} M in **1**, was placed in a UV cell fused to a Teflon-brand stopcock. The solution was brought to 60 °C in the temperature control unit of the UV spectrometer and spectra were recorded at regular intervals so that 15–20 points were collected over 4–5 half-lives of the reaction.

The intensity of the absorption at $\lambda = 444$ nm was recorded from each spectrum. The data thus obtained were used to plot ln $(I_t - I_\infty)$ vs. time. The end point used was that which gave the best correlation coefficient in the least-squares fit to a straight line, but these were not significantly different from experimental values. In all runs the correlation coefficient r was greater than 0.999.

Reaction of 1 with Varying Concentrations of $CpMo(CO)_3H$. A stock solution of **1** (0.0156 M) and ferrocene (0.0059 M) in C_6D_6 was prepared. Varying measured amounts of $CpMo(CO)_3H$ were charged into different NMR tubes and were each dissolved in 0.45 mL of the stock solution. The tubes (7 in all) were kept together at room temperature for 2 days at which point an NMR spectrum of each solution was recorded. The spectra consisted of 4 pulses with a long (20 s) delay between each one, in order to assure complete relaxation and therefore accurate integration. The yield of **4** was determined in each case by integration of the methyl resonancce of **4** vs. ferrocene, correcting for the extent of conversion of **1**.

(30) Zachariesen, W. H. *Acta Crystallogr.* **1963**, *16*, 1139.

Reaction of 1 with $CpMo(CO)_3H$ in Solvents of Varying Viscosity. In the drybox, four different 10-mL round-bottom flasks were each charged with carefully weighed out amounts of **1** (21.7 mg, 0.066 mmol) and $CpMo(CO)_3H$ (98.4 mg, 0.40 mmol). One of the appropriate solvents, either benzene, *p*-xylene, *o*-xylene, or Nujol, was measured out by using a graduated pipet (2.00 mL) and added to each of the flasks. The solutions were allowed to stir at 20 °C for 2 days at which point they were chromatographed on neutral alumina II. Elution with hexane yielded unreacted $CpMo(CO)_3H$ and further elution with benzene gave a dark fraction containing both ethylidene **4** and cluster **5**. Solvent was removed from the latter fraction by vacuum transfer and the residue was analyzed by ^{1}H NMR using ferrocene as an internal quantitative standard.

Reaction of 1 with $CpMo(CO)_3H$ under CO. In the drybox a solution of **1** (6.6 mg, 0.02 mmol) and $CpMo(CO)_3H$ (24.6 mg, 0.10 mmol) in C_6D_6 was divided evenly between two NMR tubes fitted with ground glass joints. One of the tubes was sealed under vacuum, and to the other 400 torr of CO was admitted and the tube was sealed at −196 °C (giving approximately 2 atm CO at room temperature). The tubes were placed in the probe of the NMR spectrometer preheated to 60 °C, and 1-pulse spectra were taken at 5-min intervals. The disappearance of **1** was monitored by integrating the resonance due to the vinylidene CH_2 group (δ 6.1) against that of C_6D_5H in the solvent. Measurments were taken over 3 half-lives, and a pseudo-first-order plot gave acceptable straight lines ($r > 0.98$ in both cases) with slopes equal to k_{obsd}.

Acknowledgment. We are grateful for financial support of this work by a grant (including a 2-year creativity extension) from the National Science Foundation (Grant No. CHE79-26291). We also appreciable helpful discussions with Profs. G. L. Closs, J. Halpern, and J. Norton. The crystal structure analyses were performed by Dr. F. J. Hollander, staff crystallographer at the UC Berkeley X-ray Crystallographic Facility (CHEXRAY). Funds for the analysis were provided by the above NSF grant; partial funding for the equipment in the facility was provided by the NSF through Grant No. CHE79-07027. R.G.B. acknowledges a research professorship (1982–1983) from the Miller Institute for Basic Research at UC Berkeley and a Sherman Fairchild Distinguished Scholarship from the California Institute of Technology (January–June 1984). E.N.J. acknowledges a Regents Fellowship from the University of California (1984–1985).

Registry No. 1, 88336-67-8; **1**-d_2, 95248-88-7; **2**, 88336-69-0; **3**, 95217-17-7; **4**, 88336-70-3; **5**, 88343-62-8; 6, 95217-18-8; $[CpCo(CO)]_2$, 58496-39-2; $CpCo(CO)_2$, 12078-25-0; CpCo(CO), 73740-50-8; $[CpW(CO)_3]_2$, 12091-65-5; $Na[Cp_2Co_2(CO)_2]$, 62602-00-0; $CpMo(CO)_3H$, 12176-06-6; $CpMo(CO)_2(PPh_3)H$, 33519-69-6; $CpMo(CO)_2(PMe_3)H$, 78392-89-9; $CpCr(CO)_3H$, 36495-37-1; $CpW(CO)_3H$, 12128-26-6; $(CO)_5MnH$, 16972-33-1; $CpMo(CO)_3D$, 79359-05-0; $NaMo(CO)_3Cp$, 12107-35-6; $NaMn(CO)_5$, 13859-41-1; $H_2C{=}CBr_2$, 593-92-0; C_6H_6, 71-43-2; 1,1,2-tribromoethane, 78-74-0; *p*-xylene, 106-42-3; *o*-xylene, 95-47-6; vinyl bromide, 593-60-2.

Supplementary Material Available: Positional and thermal parameters of the refined atoms, the positions of the hydrogen atoms, general temperature factor expressions and their esds, a listing of the values of F_o and F_c, and raw interatomic distances and angles for **5** and **6** (59 pages) (published in the microfilm edition of the journal, available in many libraries). Ordering information is given on any current masthead page. Analogous data for the structure determination on complex **1** are given in the supplementary information provided with ref 8.